BEHAVIOUR OF EMBEDDED BRAGG GRATING SENSORS

J.L. Esteves[1], C.A. Ramos[2], R. de Oliveira[3]

[1] Departamento de Engenharia Mecânica e Gestão industrial (DEMEGI)
Faculdade de Engenharia da Universidade do Porto (FEUP).
Rua Dr. Robert Frias s/n, 4200-465 Porto, Portugal.
email: jesteves@fe.up.pt

[2] Departamento de Física, Instituto Superior de Engenharia do Porto (ISEP).
Rua Dr. António Bernardino de Almeida 431, 4200-072 Porto, Portugal.
email: cramos@isep.ipp.pt

[3] Instituto de Engenharia Mecânica e Gestão industrial (INEGI),
Unidade de Materiais Compósitos
Rua do Barroco, 174, 4465-591 Leça do Balio, Portugal.
email: rcosta@inegi.up.pt

ABSTRACT

In this paper, an attempt is made to evaluate the performance of fibre Bragg grating sensors, when embedded into a carbon composite plate whose final purpose is to be used as strain sensors for a structure in analyse bonding it at its surface. The strain response of the composite sensor plate to longitudinal strain is compared to electrical strain gage's. A three dimensional finite element analysis is also proposed to understand the relation between the strain measured by the FBG sensor and the strain imposed to the composite specimen submitted to tensile loading. The benefits and drawbacks of using such sensor plates are discussed.

INTRODUCTION

Structural health monitoring of composite structures may be accomplished from strain measurement. In the composite smart structures development, the optical fibre Bragg grating (FBG) sensors offer various benefits compared to their electric counterparts for strain measurement (Udd, 1995). Most important is their immunity to electromagnetic interference, which enables their application under difficult environmental conditions (Krohn, 2000, Zhou et al., 2002). Their low dimensions and low weight also facilitates their embedment into composite materials structures, without affecting their structural integrity (Measures, 1995). However, FBG sensors are most commonly bounded to the structure surface using a polyamide tape or adhesives. But, it is not rare that such sensors break during their life due to the brittle nature of silica.

Their embedment in a composite plate permits to guarantee their safety. Such composite sensor plate has been proposed (Ramos et al., 2006) to be bonded to structures in analysis made from the embedment of a FBG sensor in weaved carbon fibre reinforced plastic (CFRP) composite plates. A weaved architecture was chosen to guarantee a good compromise, being

resistant enough to significant bending and torsion displacement for a low sensor plate thickness.The bounding of such CFRP specimen to the structure to be analysed shall induce alterations on the structure behaviour. In this paper an experimental and a numerical analysis are proposed to understand the behaviour of such FBG sensor plate and its efficiency as potential longitudinal strain sensor. The sensor plate was surface mounted to a glass fibre reinforced plastic (GFRP) composite specimen submitted to tensile loading. Its longitudinal strain answer was compared to the answer of conventional electrical strain gages (SG).

FIBRE BRAGG GRATING SENSOR

FBG are formed when a permanent periodic variation of the index of refraction of the core is created along a section of an optic fibre, by exposing the optic fibre to an interference pattern of intense ultra-violet light (Krohn, 2000, Morey, 1989). The photosensitivity of silica glass permits the index of refraction in the core to be increased by the intense laser radiation. If the optical fibre with a FBG is illuminated by a broadband light source, the grating diffractive properties promote that only a very narrow wavelength band is reflected back. The central wavelength of this band can be represented by the well known Bragg condition:

$$\lambda_B = 2n\Lambda \tag{1}$$

where λ_B is the centre wavelength, n is the effective index of the guided mode and Λ is the period of the index modulation. FBG sensors are sensitive to both strain and temperature. The FBG resonance wavelength varies with strain and temperature changes experienced by the fibre. To recover the strain, it must be decoupled from the temperature variation, ΔT. The temperature must then be measured separately. This can be done using a simple thermocouple or a second FBG, for example. The wavelength shift, induced by a longitudinal strain variation $\Delta \lambda_B$ is then given by (Morey, 1989)

$$\Delta \lambda_B = \lambda_B \left(\frac{1}{\Lambda} \frac{\partial \Lambda}{\partial \varepsilon} + \frac{1}{n} \frac{\partial n}{\partial \varepsilon} \right) \Delta \varepsilon = \lambda_B \left(1 - p_e \right) \Delta \varepsilon \tag{2}$$

where p_e is the photoelastic coefficient of the fibre. For a silica fibre, the wavelength-strain sensitivity is typically around 1.15 $pm.\mu\varepsilon^{-1}$, for a Bragg wavelength centred at 1555 nm (Hill, 1993).

EXPERIMENTAL PROCEDURE

Material

The CFRP sensor plate was fabricated using carbon-epoxy pre-impregnated sheets (SEAL CC206, twill 2/2). The prepegs were cut, with the dimensions 100×20 mm^2, and laid up by hand, the optical fibre was placed in the mid-plane of the laminate along the 100 mm direction. After lay-up, the CFRP laminate was vacuum-bagged and placed in an autoclave, where it was slowly heated to 130 ºC under internal vacuum (0.85 bar) and 0.1 MPa of external pressure. After holding for 1 hour at this condition, the laminate was slowly cooled in the autoclave. The laminate was trimmed along side edges to its final dimensions, and with a thickness of 0.4 mm.

The GFRP tensile specimen, with the dimensions $300 \times 50 \times 3.3$ mm^3, was manufactured from four layers of equilibrated weaved E glass fibre tissues (50 % of fraction of fibre in 0 and 90 directions) impregnated by epoxy resin by hand lay-up assisted by vacuum (0.85 bar).

FBG sensor

FBG sensors 10 mm long, with a nominal resonance wavelength of 1552.2 ± 0.5 nm after annealing, with a strain sensitivity of $0.77 \pm 0.05.10^{-6} \mu\varepsilon^{-1}$, were written in SMF - 28e$^®$ optical fibres from CORNINGS. The FBG data was acquired during tensile test. The optical fibres were illuminated through a broadband optical source. The variation of the FBG central wavelength was recorded using a BraggScope dynamic measurement unit for FBG sensors from FIBERSENSING SA .

Mechanical testing

Monotonic tensile tests were performed, at room temperature (23±2 ºC and 50±5 % RH), on the GFRP specimen using an INSTRON® Model 4208 universal testing machine, according to the ISO 527 standard. The speed test was controlled by displacement to 0.1 mm.min^{-1}. An acquisition system from HBM$^®$- Spider 8 was used to collect the applied load, the crosshead displacement and the strain values obtained by six electric SGs that were located at the GFRP specimen and CFRP plate surfaces as described in figure 1. The answer of the SG - H was compared to the strain value provided by the FBG, whereas the other SG were used to the analysis of the influence of the CFRP plate on the GFRP specimen behaviour.
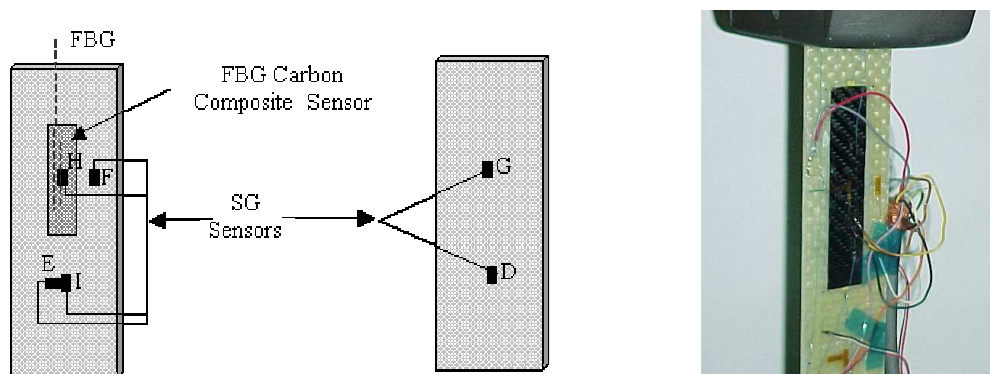
Fig. 1 SG location and tensile test set-up

FINITE ELEMENT ANALYSIS

A numerical model based on the finite element method was developed to verify the sensor plate behaviour when bounded to the surface of the GFRP composite specimen. The analysis was executed using the commercial software ABAQUS^{TM}. 20-nodes quadratic brick elements were used to generate the mesh.

The following basic assumptions have been made to simplify the problem:
- The optical fibre, CFRP host and GFRP specimens are linear elastic.
- The host material is supposed homogenised and orthotropic.
- Plane stress state.
- The study is limited to the small displacement and small strain case

The weaved microstructure of CFRP and GFRP plates is neglected for the three-dimensional FE model of the sensor plate. E_1, E_2 and ν_{12} were measured experimentally for the CFRP and GFRP laminas. For the other mechanical properties, equivalent properties were determined using the ESAComp software for the analysis and design of composite laminates and laminated structural elements. The obtained properties are summarized in table1.

Material	E_1 [GPa]	E_2 [GPa]	E_3 [GPa]	ν_{12}	ν_{13}	ν_{23}	G_{12} [GPa]	G_{13} [GPa]	G_{23} [GPa]
Carbon-epoxy twill	43.91	43.91	4.46	0.024	0.325	0.325	2.29	1.68	1.68
Glass-epoxy twill	19.22	19.22	3.72	0.133	0.32	0.32	2.23	1.95	1.95
Adhesive Epoxy resin	1.20	1.20	1.20	0.33	0.33	0.33			

Table 1: Material properties

The maximum load applied to the GFRP specimen was set to 2000 N which corresponds to the load applied during the tensile test. A FEM modelling of the GFRP specimen was made considering that the CFRP plate was not exactly located at the middle of the GFRP specimen. The geometry and boundary conditions are summarised in figure 2. Dimensions are provided in millimetres. The GFRP specimen was considered to be fixed at one extremity and loaded at the opposite along the length direction. This approximation was close to the real case.
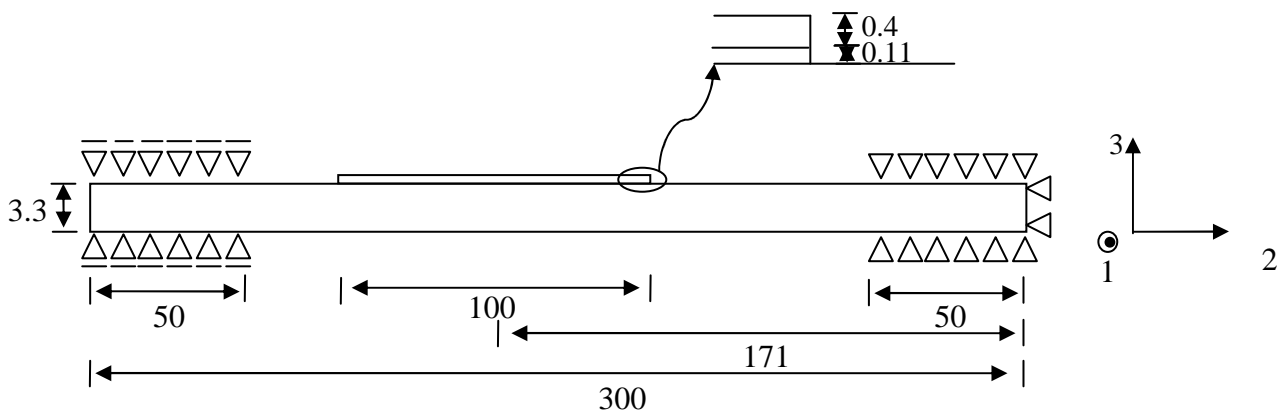
Fig. 2 Geometry and boundary conditions

RESULTS

The answers of the FBG sensor and the SG – H, mounted at the surface of the CFRP plate, along the tensile test, are reported in figure 3. Similar sensibility was noticed for both strain sensors. This is emphasised by their behaviour at tensile machine grip closure (figure 3 (a)). Due to the high sampling rate of the FBG interrogation unit, significant fluctuations on the optical signal were observed. This can easily be removed performing an average of values. In figure 3 (b) is represented the correlation between the two sensors answers. A good relationship is observed. The correlation is underlined when performing a linear fitting of the FBG answer.

(a)   (b)
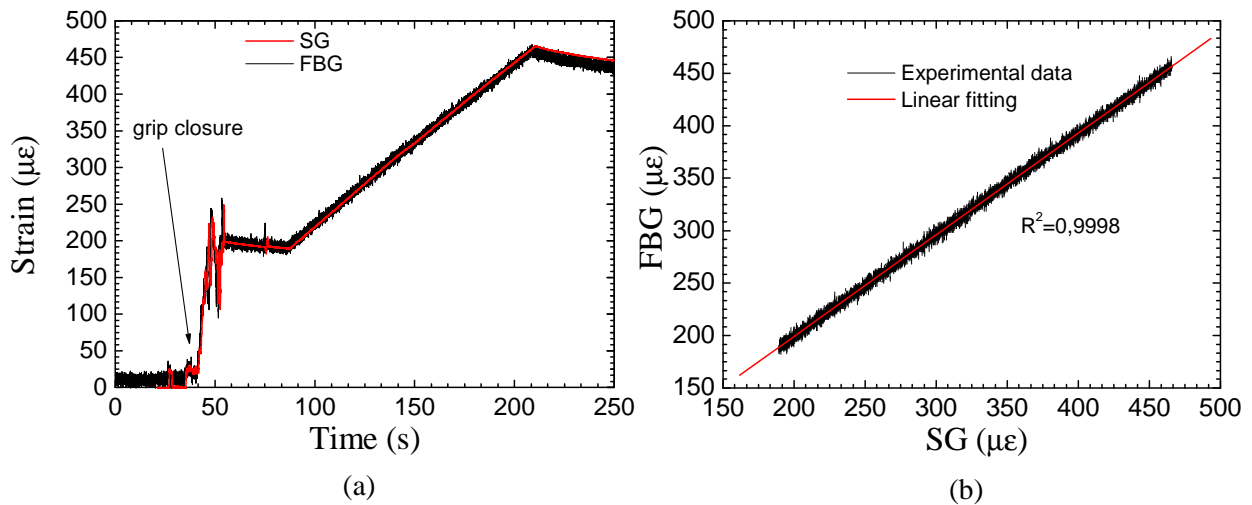
Fig. 3 Comparison of FBG and SG sensors answers along tensile test

In figure 4 and 5 are represented the calculated longitudinal strain values along the specimen length. Strains values have been amplified for better visualization of the influence of the CFRP sensor plate on the mechanical behaviour of the GFRP specimen. This permits to underline the reinforcement effect of the CFRP sensor plate in the specimen's side it is bounded to, resulting in a slight flexion of the GFRP specimen.
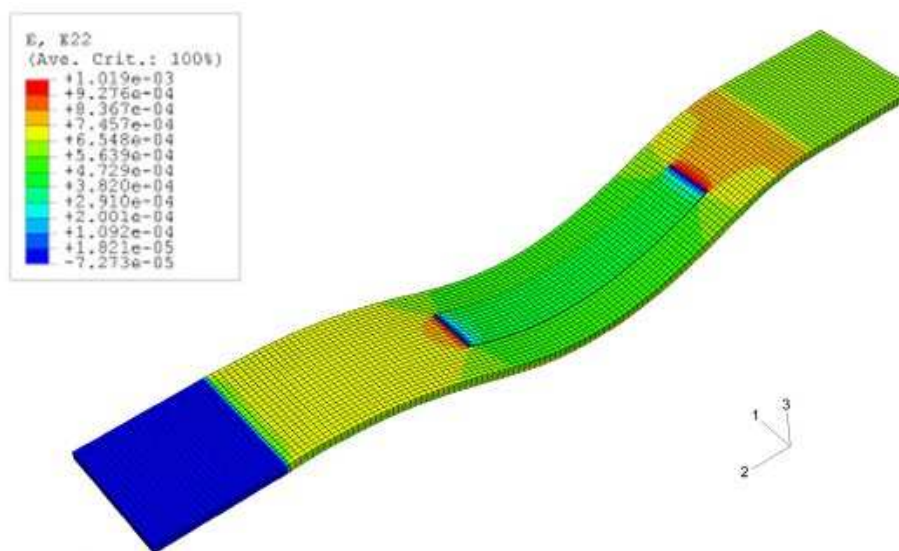
Fig. 4 Calculated longitudinal strain.

The strain values measured by the SG at the different locations are reported in table 2 and compared to the calculated value by the FEM model. Values given by the model correspond are not an average value but rather the strain values at a single node. The so-obtained values are of the same order of magnitude confirming the accuracy of the model. However, the values obtained by the FEM model at location I and G are significantly higher to the one measured.
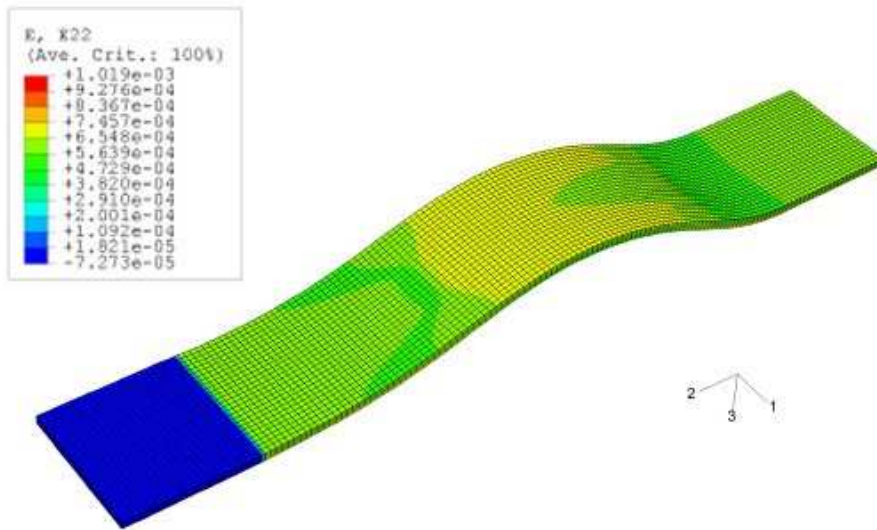
Fig. 5 Calculated longitudinal strain.

Measure location	Electrical strain gage [$\mu\varepsilon$]	Finite element model [$\mu\varepsilon$]
D	614	615.6
E	-78	-87
F	513	491.8
I	588	687.1
G	490	611.6
H	454	440.7
CFRP	454.2 (FBG)	441

Table 2: Strain measures and numerical strain values

This difference is observed all along the tensile test (figure 6). When comparing the strain values at position F, H and I the same tendencies, were observed for experimental and numerical values. The differences may be due to some variation between the considered boundary conditions and the ignorance of the weaved nature of GFRP reinforcement

(a)

(b)
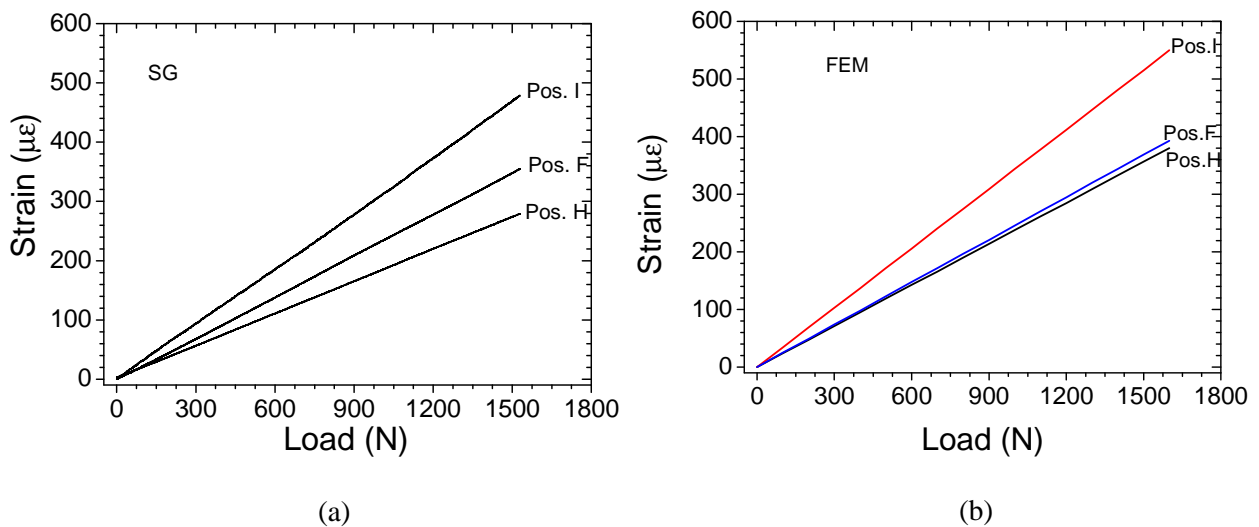
Fig. 6 Longitudinal strain along test

It can be observed that CFRP plate sensor suffers an inferior deformation than the GFRP specimen, possibility due to the bigger rigidity of the CFRP plate, and to the very low rigidity of the adhesive used in the bond of the sensory plate. This last one may act as a filter not transmitting the totality of the deformation at the surface of the GFRP specimen to the sensor plate. The strain value at the surface of the CFRP plate revealed to be similar to the strain value in the middle plan of the sensor plate as it was possible to observe in the experimental test.

A sensor calibration is then relevant. In figure 7 is represented the strain values obtained by the FEM model for the single GFRP plate without the surface bounded CFRP plate. This allows to recover the exact strain values from the one provided by the CFRP sensor plate.
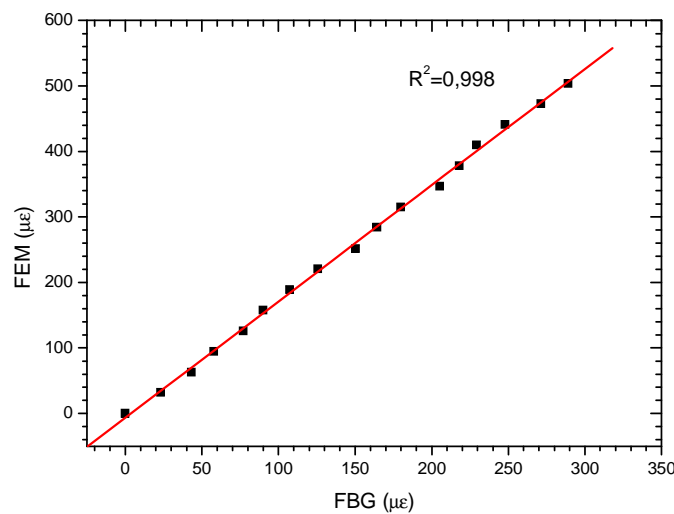
Fig. 7 FBG sensor plate calibration

CONCLUSIONS

It can be observed that the CFRP plate sensor suffers an inferior deformation than the GFRP structure in analysis, possibility due to the bigger stiffness of the CFRP plate, and to the very low stiffness of the adhesive used for the sensor plate bonding. This last one may act as a filter not transmitting the totality of the deformation at the GFRP structure's surface to the sensor plate. It is then desirable to produce sensory plates constituted of a composite material with lower stiffness than the structure to be monitored. However the sensor provides a good answer and the strain field may be recovered after performing a calibration. Reinforcement effect can be decreased through sensor plate dimensions adjustments.

ACKNOWLEDGEMENTS

REFERENCES

Hill K.O., Malo B., Bilodeau F., Johnson D.C., Albert J., Bragg gratings fabricated in monomode photosensitive optical fiber by UV exposure through a phase mask. Appl. Phys. Lett., 62; 1993 pp. 1035-1037.

Krohn D.A. Fibre Optic Sensors, Fundamentals and Applications. Instrument Society of America, third edition, ISBN 1-55617-714-3, 2000.

Measures R. Fiber Optic Strain Sensing. Smart Structures, Udd E. Ed., ISBN 0-471-55448-0, 1995 pp. 171-247.

Morey W.W., Meltz G., Glenn W.H. Fibre optic bragg grating sensors. Fiber Optic and Laser Sensors VII, in Proc. SPIE 1169, Boston, USA, 1989 pp. 98-107.

Ramos C.A., Esteves J.L., Silva R.A., Marques A.T. Analysis of composite structures behaviour with embedded grating sensors. Materials Science Forum; 514-516; 2006 pp. 614-618

Udd: E. Fibre Optic Smart Structure Technology. In Fibre Optic Smart Structures, John Wiley & Sons, Inc., ISBN 0-471-55448-0, 1995 pp. 5-21.

Zhou G., Sim L.M. Damage detection and assessment in fibre-reinforced composite structures with embedded fibre optic sensors-review. Smart Mat. Structures; 11, 2002, pp. 925-939.